Surface Functionalization | Hot Paper

International Edition: DOI: 10.1002/anie.201506888
German Edition: DOI: 10.1002/ange.201506888

Surface-Specific Functionalization of Nanoscale Metal–Organic Frameworks

*Shunzhi Wang, William Morris, Yangyang Liu, C. Michael McGuirk, Yu Zhou, Joseph T. Hupp, Omar K. Farha, and Chad A. Mirkin**

Abstract: *A method for modifying the external surfaces of a series of nanoscale metal–organic frameworks (MOFs) with 1,2-dioleoyl-sn-glycero-3-phosphate (DOPA) is presented. A series of zirconium-based nanoMOFs of the same topology (UiO-66, UiO-67, and BUT-30) were synthesized, isolated as aggregates, and then conjugated with DOPA to create stably dispersed colloids. BET surface area analysis revealed that these structures maintain their porosity after surface functionalization, providing evidence that DOPA functionalization only occurs on the external surface. Additionally, dye-labeled ligand loading studies revealed that the density of DOPA on the surface of the nanoscale MOF correlates to the density of metal nodes on the surface of each MOF. Importantly, the surface modification strategy described will allow for the general and divergent synthesis and study of a wide variety of nanoscale MOFs as stable colloidal materials.*

Metal–organic frameworks (MOFs) and infinite coordination polymers (ICPs) are porous materials composed of organic ligands coordinated to metal containing units.[1] The pore sizes and functionalities of these materials can be deliberately modulated through the choice of organic ligands and metal-containing units. This structural tailorability has led to the study of these materials for a variety of applications, including gas storage,[2] chemical sensing,[3] membrane separations,[4] and catalysis.[5] Against this backdrop, there has been significant interest more recently in the synthesis of these materials on the nanoscale, in particular because the crystallite shape and size uniformity of nanoscale MOFs can be precisely controlled and tailored. Additionally, these materials show enhanced small-molecule uptake and release kinetics, making them promising materials for applications in catalysis[6] and biology.[7] A pivotal feature of designing MOFs for such applications, especially on the nanoscale, is a firm understanding of the underlying MOF structure, particularly that of the surface.

MOFs are crystalline structures, and therefore, their bulk structure is well-understood as a result of single-crystal studies and refinement of powder X-ray diffraction (PXRD) data. Recently, there has been significant effort aimed at realizing generalizable methods to post-synthetically functionalize the bulk MOF structure, such as coordination at activated metal-binding sites and linker modification.[8] However, the surface chemistry of MOFs likely deviates from the bulk structure, owing to the presence of additional vacant coordination sites, surface defects, and the binding of synthetic modulators.[9] Despite this expected deviation in structure from bulk to surface, only a few studies have focused on the characterization and modulation of the external surface of MOFs.[10] Importantly, it has been repeatedly shown that for nanoscale materials (for example, metal nanoparticles) surface chemistry tends to dictate physical properties and chemical function.[11] Therefore, for the advancement and application of MOFs on the nanoscale, the development of general methods for surface functionalization must be developed. In this vein, we describe herein a method for the facile surface functionalization of a series of isoreticular, chemically stable nanoMOFs with the phosphate-containing amphiphilic ligand DOPA (Scheme 1c) by well-defined coordination chemistry. Additionally, we demonstrate the ability to control the density of surface ligands, as well as solvent compatibility of the MOF, all while preserving the structural integrity and porosity of the MOF architecture.

To carry out this study, we chose a family of isoreticular MOFs with different linker lengths, in which the bulk structure was well-characterized, the framework was chemically stable under various conditions, and the modular nanoscale synthesis had been realized.[12] Therefore, we selected three zirconium-based frameworks with the same underlying topology, namely UiO-66 ($Zr_6O_4(OH)_4(BDC)_6$),[13] UiO-67 ($Zr_6O_4(OH)_4(BPDC)_6$),[13] and BUT-30 ($Zr_6O_4(OH)_4(EDDB)_6$).[14] Importantly, within this family, the density of metal nodes decreases as a function of increasing organic ligand length (Scheme 1a,b). These three frameworks were functionalized with DOPA to give DOPA–UiO-66, DOPA–UiO-67, and DOPA–BUT-30 (Scheme 1c). DOPA was selected as a ligand because it was expected to coordinate strongly to the Zr^{IV} metal-containing units, but, importantly, not too strongly as to disturb the underlying coordination framework of the MOF.[15] Upon functionalization with DOPA, the surface ligand density, as well as the bulk MOF

[*] S. Wang,[+] Y. Liu, C. M. McGuirk, Prof. J. T. Hupp, Prof. O. K. Farha, Prof. C. A. Mirkin
Department of Chemistry
Northwestern University, Evanston, IL (USA)
E-mail: chadnano@northwestern.edu
W. Morris,[+] Prof. C. A. Mirkin
International Institute for Nanotechnology
Northwestern University, Evanston, IL (USA)
Y. Zhou, Prof. C. A. Mirkin
Department of Material Science and Engineering
Northwestern University, Evanston, IL (USA)
Prof. O. K. Farha
Department of Chemistry, King Abdulaziz University
Jeddah (Saudi Arabia)
[+] These authors contributed equally to this work.

Supporting information for this article is available on the WWW under http://dx.doi.org/10.1002/anie.201506888.

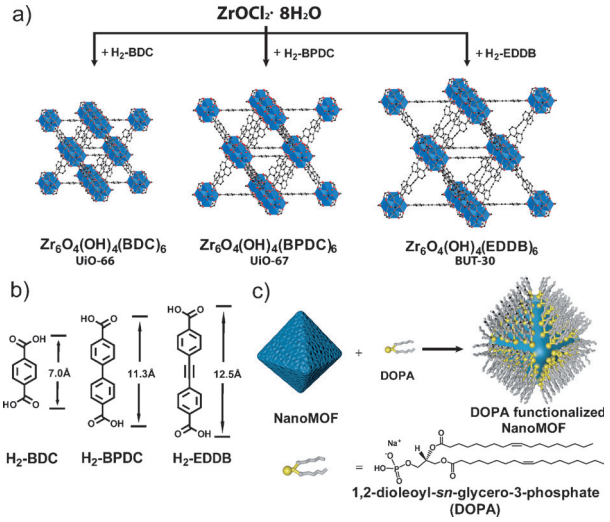

Scheme 1. Synthesis and DOPA functionalization of a series of zirconium nanoMOFs with the same underlying topology. a) The preparation of UiO-66, UiO-67, and BUT-30. b) The series of ligands utilized in the synthesis of nanoscale MOFs and their lengths. H_2-bdc = terephthalic acid ($C_6H_6O_4$), H_2-bpdc = biphenyldicarboxylic acid ($C_{14}H_{10}O_4$), H_2-eddb = 4,4′-(ethyne-1,2-diyl)dibenzoic acid ($C_{16}H_{10}O_4$). c) The functionalization for MOF nanoparticles utilizing DOPA.

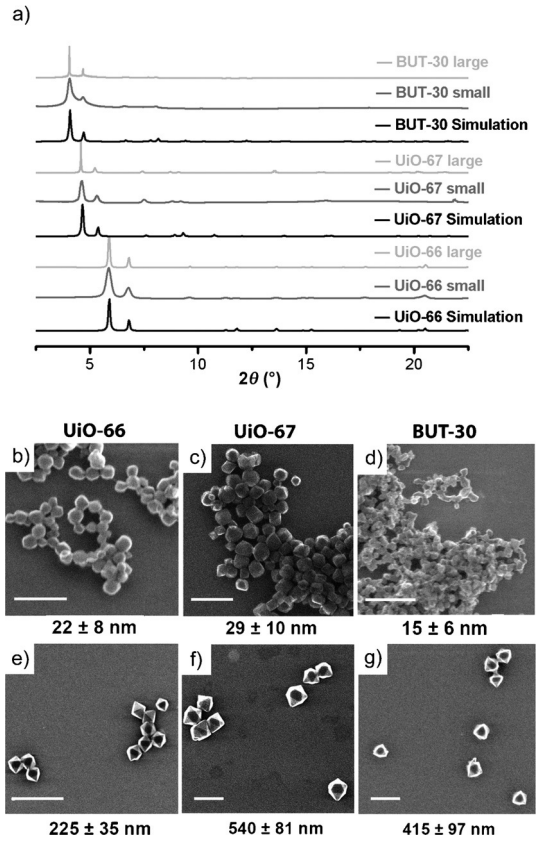

Figure 1. Powder X-ray diffraction (PXRD) patterns and scanning electron microscopy (SEM) images of the as-synthesized nanoMOFs. a) Simulated and experimental PXRD patterns of UiO-66, UiO-67, and BUT-30. SEM images of b,e) UiO-66, c,f) UiO-67, and d,g) BUT-30. Scale bar: 100 nm for (b–d) and 1 μm for (e–g).

porosity and structure, were evaluated. Additionally, the colloidal stability of the nanoMOFs was determined to be dramatically altered upon DOPA surface functionalization. Namely, it was found that unfunctionalized UiO-66, UiO-67, and BUT-30 aggregate extensively in nonpolar solvents; however, after surface modification with DOPA, nanoMOF constructs can easily be dispersed and suspended in solvents with low polarity. From BET surface area measurements, we show that the porosity of the MOFs is maintained post-functionalization. Importantly, for the application of MOFs on the nanoscale, this general method for surface modification, based on straightforward coordination chemistry, allows for the modulation of the density of surface ligands. Thus, the colloidal properties of these constructs can be finely tuned.

The isoreticular zirconium nanoMOFs were synthesized under solvothermal conditions utilizing acetic acid to modulate crystallite size.[8] For example, 22 ± 8 nm UiO-66 particles were synthesized from the reaction of $ZrOCl_2 \cdot 8H_2O$ (21 mg, 65.1 μmol) with terephthalic acid (50 mg, 0.3 mmol) modulated by 0.3 mL acetic acid in 4 mL DMF at 90 °C for 18 h. For each structure, the acetic acid concentration was modulated to access the desired nanoscale crystallite parameters. PXRD analysis was utilized to confirm the bulk structure of each synthesized MOF (Figure 1 a). All three MOFs possess the expected **fcu** topology, with pore size and the density of zirconium units being determined by linker length (Scheme 1 b). For each MOF, small nanoparticles (< 30 nm) and large nanoparticles (> 200 nm) were synthesized, with the size being confirmed by scanning transmission electron microscopy (STEM; Figure 1 b).

After the synthesis and characterization of the nanoscale zirconium-based MOF family, the particles were functionalized with DOPA. First, to remove the excess and encapsulated DMF remaining from the solvothermal synthesis, UiO-66, UiO-67, and BUT-30 MOF nanoparticles were solvent-exchanged by several rounds of centrifugation and subsequently redispersed in chloroform (see the Supporting Information). Owing to their hydrophilicity, the nanoMOFs were observed to aggregate extensively in the chloroform suspension. To disperse the nanoparticles, excess DOPA (sodium salt) was added to the MOF aggregates, which were subsequently sonicated for one hour at room temperature, then left on a shaker overnight. The resulting DOPA–nanoMOF conjugate was then washed with chloroform three times until no excess DOPA could be detected in the resulting supernatant via inductively coupled plasma atomic emission spectroscopy (ICP-AES; see the Supporting Information). Additionally, by using a large excess of DOPA, we assume that the surface is coordinatively saturated by the ligand (see below). Importantly, through PXRD studies and STEM, we were able to confirm that the framework crystallinity and crystallite size were maintained after functionalization (see the Supporting Information).

To confirm the presence of DOPA on the MOFs, multiple spectroscopy techniques were used. First, IR spectroscopy was carried out for each sample. IR spectroscopy of the DOPA–nanoMOF conjugates revealed alkane (C–H) and

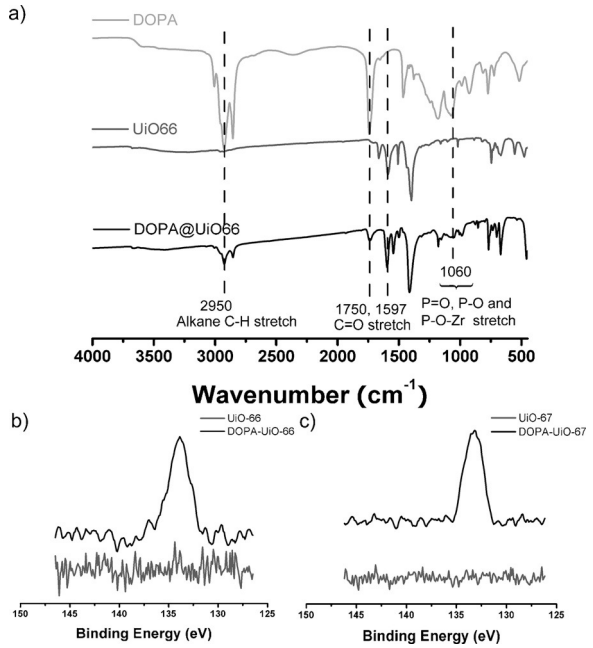

Figure 2. IR and XPS analysis of DOPA–nanoMOF. a) Comparison of an unfunctionalized DOPA molecule (top), UiO-66 particles (middle), and DOPA–UiO-66 (bottom). b) XPS spectra of UiO-66 and UiO-67 before (gray) and after (black) DOPA functionalization.

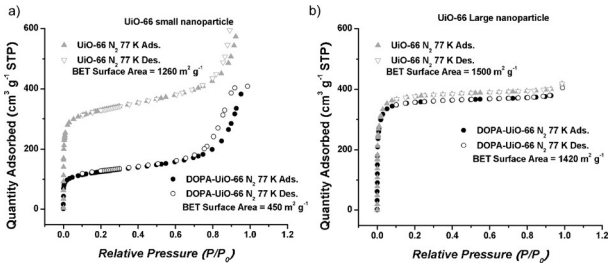

Figure 3. The impact of DOPA functionalization on porosity and colloidal stability. BET adsorption isotherm before and after DOPA functionalization for a) 25 nm UiO-66, b) 225 nm UiO-66.

carbonyl (C=O) vibrations at 2950 cm^{-1} and 1597 cm^{-1}, respectively, which correlate well with the spectra of free DOPA, and are not present in the IR spectra of the unmodified MOFs (Figure 2a). Additionally, X-ray photoelectron spectroscopy (XPS) shows a peak at 134 eV, confirming the presence of phosphate in the DOPA-functionalized samples (Figure 2b,c). Finally, $^{31}P\{^{1}H\}$ magic angle spinning (MAS) NMR spectroscopy was performed to directly examine coordination of the phosphate group of DOPA to the zirconium cluster. For the DOPA-functionalized nanoMOF, a broad resonance at −3.2 ppm, along with two symmetric satellite resonances (58.1 ppm and −65.3 ppm) was observed. In contrast, the free DOPA molecule exhibits a single sharp resonance at 2.1 ppm (Supporting Information, Figure S9). Taken together, these results strongly suggest that the phosphate ligands coordinate to the zirconium oxide nodes on the external surface of the MOF nanoparticle.[16]

To characterize the porosity of the DOPA-functionalized MOF nanoparticles, we performed N_2 isotherms and evaluated their surface area by BET analysis (Figure 3). Prior to the surface area measurements, the samples were activated to remove solvent from the pores of the MOF (see the Supporting Information). The N_2 adsorption isotherm for each nanoMOF at 77 K exhibits type-I behavior. In each case, the larger MOF crystallites (>200 nm), which were realized by using higher modulator concentrations (see the Supporting Information for solvothermal reactions conditions), exhibit higher surface area when compared to the smaller MOF nanocrystals of the same underlying structure. This finding correlates well with previous studies, which show that the surface area of UiO-66 is dependent on the defects induced by modulator used in the synthesis.[17] The gradual increase in N_2 uptake at high P/P_o values (Figure 3a) is most likely due to N_2 condensation in interparticulate voids generated by nanocrystallite packing. After DOPA functionalization, the N_2 isotherms show that each MOF maintained its porosity, suggesting that the pores of each MOF are still accessible (For N_2 adsorption isotherms of UiO-67, see the Supporting Information). Interestingly, in the case of small nanocrystallites, a significant decrease in porosity was observed, whereas the larger nanocrystallites demonstrated porosities much closer to the unfunctionalized structures (Figure 3). For example, in UiO-66 a 64% and 5% drop in surface area was seen for the small (<30 nm) and large (>200 nm) nanocrystals, respectively. The apparent difference in porosity change between small and large nanoMOF samples upon DOPA surface functionalization can be attributed to the disparity in external surface-to-volume ratios between the two particle sizes. In the case of small nanoparticles, approximately 50% of the zirconium secondary building units are found within one unit cell of the external surface, which is in stark contrast to the large nanoparticles in which less than 5% of the zirconium units are this close to the surface. This significant difference leads to a higher weight percentage of DOPA in samples of small crystallites, thus reducing their gravimetric surface area. This trend is observed for all three MOF architectures. Additionally, these results support the hypothesis that DOPA functionalization is limited to the external surface of each MOF, as no surface area would be expected if the crystal was completely modified.[18]

Quantitative analysis of DOPA coverage for each nanoMOF architecture was conducted via ICP-AES. By measuring the phosphorous and zirconium amount, we determined the DOPA loading of each nanoMOF sample from the ratio of Zr and P (Figure 4a). These results showed that UiO-66 had the highest DOPA loading (212 ± 57 pmol cm^{-2}), and BUT-30 had the lowest (83 ± 20 pmol cm^{-2}). This significant difference in loading between UiO-66 and BUT-30 supports the hypothesis that DOPA binds to the Zr surface units, as decreasing the density of these Zr surface sites results in lower surface coverage of DOPA ligands (Figure 4a). To verify the results of the above ICP-AES study, the density of nanoMOF surface functionalization with a dye-labeled analogue of

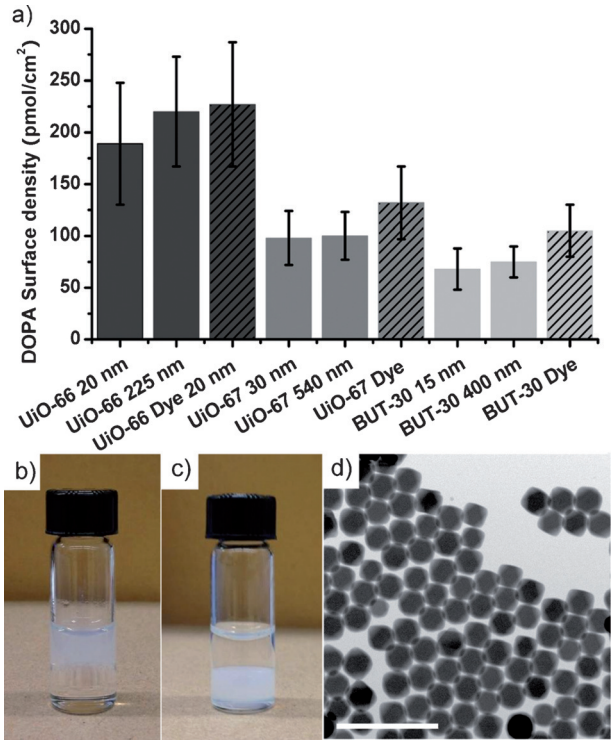

Figure 4. a) DOPA surface density for different-sized UiO-66, UiO-67, and BUT-30 MOF nanoparticles. Values for solid columns were determined by ICP-AES, and values for diagonally striped columns were determined by UV/Vis. b) Digital photograph showing nanoMOFs suspended in an aqueous phase after being transferred to c) a chloroform phase after DOPA functionalization and d) a SEM image of drop-casted colloidally stable DOPA–UiO-66 in $CHCl_3$. Scale bar: 1 μm.

DOPA, 1-oleoyl-2-{12-[(7-nitro-2-1,3-benzoxadiazol-4-yl)amino]dodecanoyl}-*sn*-glycero-3-phosphate (NBD-DOPA), was measured by UV/Vis absorption studies at 460 nm (see the Supporting Information for details). Importantly, this absorbance study strongly agrees with the loading densities determined by ICP-AES (Figure 4a). The synchronous results of the ICP-AES and absorption studies support the hypothesis that DOPA binding is limited to the surface, as the observed loading densities are in close alignment with an average of two DOPA molecules coordinated to each of the surface metal-containing units. Additionally, confocal fluorescence microscopy was performed, which verified that the dye is primarily localized on the periphery of the MOF nanoparticles (see the Supporting Information, Figure S14 for details).

The main goal of this study was to evaluate a synthetic method for promoting the colloidal stability of a series of hydrophilic MOF nanoparticles in low-polarity media by surface functionalization. Therefore, the colloidal stability of these nanoscale MOFs was evaluated before and after surface modification (Figure 4b–d). First, unfunctionalized nanoMOFs were suspended in $CHCl_3$/water mixtures. From simple visualization, the MOF nanoparticles were clearly selectively suspended in the aqueous layer (Figure 4b). In contrast, upon DOPA functionalization, the MOF nanoparticles became preferentially suspended in the $CHCl_3$ layer (Figure 4c). This binary contrast in solvent selectivity directly demonstrates that nanoparticle properties can be deliberately tailored by surface functionalization with organic ligands. Additionally, this modulation of the colloidal stability of the MOF nanoparticles was supported by SEM imaging and dynamic light scattering (DLS). SEM images of non-functionalized MOF nanoparticles that have been drop-cast from $CHCl_3$ show significant aggregation (see the Supporting Information), whereas the DOPA-functionalized MOFs exist as discrete nanoparticles when similarly drop-cast from $CHCl_3$ (Figure 4d), thus, again demonstrating the colloidal stability of the surface-modified particles in solvents with low polarity.

In summary, we have developed a general method for the selective surface functionalization of nanoMOFs, which yields the ability to disperse crystalline nanoMOFs as colloids into a variety of solvents and chemical environments. The selective coordination of organophosphates to metal binding sites on MOF nanoparticle surfaces allows for the control of ligand density and type while retaining crystallinity and permanent porosity. This strategy is general and, in principle, can be used to generate a large pool of multifunctional porous materials with surface chemistries that can be deliberately and finely tuned through judicious choice of coordination ligands. Looking forward, this work should also facilitate the integration of nanoscale MOFs into structurally tailorable particle assemblies,[19] opening the door for realizing functional materials with applications spanning optically responsive devices,[20] adsorption-based chemical sensors,[3] and plasmonic-enhanced catalysis.[21]

Acknowledgements

This material is based upon work supported by the Air Force Office of Scientific Research (AFOSR) award FA9550-14-1-0274 and the U.S. Army award W911NF-11-1-0229. O.K.F. and J.T.H. gratefully acknowledge DTRA for financial support (HDTRA1-14-1-0014). PXRD data were collected at the Dupont-Northwestern-Dow Collaborative Access Team (DND-CAT) Beamline 5-IDD at Argonne National Laboratory. Use of the DNA-CAT beamline was supported by the U.S. Department of Energy (DOE), Office of Science, Office of Basic Energy Sciences, under contract DE-AC02-06CH11357. This work made use of the EPIC facility (NUANCE Center-Northwestern University), which has received support from the MRSEC program (NSF DMR-1121262) at the Materials Research Center a program of the National Science Foundation, the State of Illinois, and Northwestern University.

Keywords: metal–organic frameworks · phosphate lipids · post-synthetic modification · surface functionalization · zirconium oxo clusters

How to cite: *Angew. Chem. Int. Ed.* **2015**, *54*, 14738–14742
Angew. Chem. **2015**, *127*, 14951–14955

[1] a) O. M. Yaghi, M. O'Keeffe, N. W. Ockwig, H. K. Chae, M. Eddaoudi, J. Kim, *Nature* **2003**, *423*, 705 – 714; b) G. Férey, *Chem. Soc. Rev.* **2008**, *37*, 191 – 214; c) O. K. Farha, J. T. Hupp, *Acc. Chem. Res.* **2010**, *43*, 1166 – 1175; d) N. Stock, S. Biswas, *Chem. Rev.* **2012**, *112*, 933 – 969.

[2] a) Y. M. Jeon, G. S. Armatas, J. Heo, M. G. Kanatzidis, C. A. Mirkin, *Adv. Mater.* **2008**, *20*, 2105 – 2110; b) O. K. Farha, A. Ö. Yazaydın, I. Eryazici, C. D. Malliakas, B. G. Hauser, M. G. Kanatzidis, S. T. Nguyen, R. Q. Snurr, J. T. Hupp, *Nat. Chem.* **2010**, *2*, 944 – 948; c) T. M. McDonald, D. M. D'Alessandro, R. Krishna, J. R. Long, *Chem. Sci.* **2011**, *2*, 2022 – 2028; d) H. Furukawa, K. E. Cordova, M. O'Keeffe, O. M. Yaghi, *Science* **2013**, *341*, 1230444.

[3] L. E. Kreno, K. Leong, O. K. Farha, M. Allendorf, R. P. Van Duyne, J. T. Hupp, *Chem. Rev.* **2012**, *112*, 1105 – 1125.

[4] a) S. Keskin, D. S. Sholl, *J. Phys. Chem. C* **2007**, *111*, 14055 – 14059; b) Y. F. Chen, J. Y. Lee, R. Babarao, J. Li, J. W. Jiang, *J. Phys. Chem. C* **2010**, *114*, 6602 – 6609; c) Y. S. Bae, O. K. Farha, A. M. Spokoyny, C. A. Mirkin, J. T. Hupp, R. Q. Snurr, *Chem. Commun.* **2008**, 4135 – 4137; d) T. H. Bae, J. S. Lee, W. L. Qiu, W. J. Koros, C. W. Jones, S. Nair, *Angew. Chem. Int. Ed.* **2010**, *49*, 9863 – 9866; *Angew. Chem.* **2010**, *122*, 10059 – 10062; e) O. K. Farha, A. M. Spokoyny, B. G. Hauser, Y. S. Bae, S. E. Brown, R. Q. Snurr, C. A. Mirkin, J. T. Hupp, *Chem. Mater.* **2009**, *21*, 3033 – 3035.

[5] a) Y. J. Cui, Y. F. Yue, G. D. Qian, B. L. Chen, *Chem. Rev.* **2012**, *112*, 1126 – 1162; b) L. E. Kreno, J. T. Hupp, R. P. Van Duyne, *Anal. Chem.* **2010**, *82*, 8042 – 8046; c) J. Lee, O. K. Farha, J. Roberts, K. A. Scheidt, S. T. Nguyen, J. T. Hupp, *Chem. Soc. Rev.* **2009**, *38*, 1450 – 1459.

[6] a) M. Oh, C. A. Mirkin, *Nature* **2005**, *438*, 651 – 654; b) A. M. Spokoyny, D. Kim, A. Sumrein, C. A. Mirkin, *Chem. Soc. Rev.* **2009**, *38*, 1218 – 1227; c) L. Q. Ma, C. Abney, W. B. Lin, *Chem. Soc. Rev.* **2009**, *38*, 1248 – 1256; d) C. Wang, K. E. deKrafft, W. B. Lin, *J. Am. Chem. Soc.* **2012**, *134*, 7211 – 7214.

[7] a) W. J. Rieter, K. M. Pott, K. M. L. Taylor, W. B. Lin, *J. Am. Chem. Soc.* **2008**, *130*, 11584 – 11585; b) S. Horike, D. Umeyama, S. Kitagawa, *Acc. Chem. Res.* **2013**, *46*, 2376 – 2384; c) C. M. Calabrese, T. J. Merkel, W. E. Briley, P. S. Randeria, S. P. Narayan, J. L. Rouge, D. A. Walker, A. W. Scott, C. A. Mirkin, *Angew. Chem. Int. Ed.* **2015**, *54*, 476 – 480; *Angew. Chem.* **2015**, *127*, 486 – 490; d) W. Morris, W. E. Briley, E. Auyeung, M. D. Cabezas, C. A. Mirkin, *J. Am. Chem. Soc.* **2014**, *136*, 7261 – 7264; e) D. M. Liu, C. Poon, K. D. Lu, C. B. He, W. B. Lin, *Nat. Commun.* **2014**, *5*, 5182.

[8] a) Z. Q. Wang, S. M. Cohen, *Chem. Soc. Rev.* **2009**, *38*, 1315 – 1329; b) A. Schaate, P. Roy, A. Godt, J. Lippke, F. Waltz, M. Wiebcke, P. Behrens, *Chem. Eur. J.* **2011**, *17*, 6643 – 6651; c) M. Kim, J. F. Cahill, H. Fei, K. A. Prather, S. M. Cohen, *J. Am. Chem. Soc.* **2012**, *134*, 18082 – 18088.

[9] a) J. Della Rocca, D. M. Liu, W. B. Lin, *Acc. Chem. Res.* **2011**, *44*, 957 – 968; b) M. Sindoro, N. Yanai, A. Y. Jee, S. Granick, *Acc. Chem. Res.* **2014**, *47*, 459 – 469; c) P. Deria, J. E. Mondloch, O. Karagiaridi, W. Bury, J. T. Hupp, O. K. Farha, *Chem. Soc. Rev.* **2014**, *43*, 5896 – 5912.

[10] a) Y. K. Hwang, D. Y. Hong, J. S. Chang, S. H. Jhung, Y. K. Seo, J. Kim, A. Vimont, M. Daturi, C. Serre, G. Ferey, *Angew. Chem. Int. Ed.* **2008**, *47*, 4144 – 4148; *Angew. Chem.* **2008**, *120*, 4212 – 4216; b) see Ref. [8a]; c) D. Y. Hong, Y. K. Hwang, C. Serre, G. Ferey, J. S. Chang, *Adv. Funct. Mater.* **2009**, *19*, 1537 – 1552; d) T. Gadzikwa, O. K. Farha, C. D. Malliakas, M. G. Kanatzidis, J. T. Hupp, S. T. Nguyen, *J. Am. Chem. Soc.* **2009**, *131*, 13613 – 13615; e) R. Makiura, S. Motoyama, Y. Umemura, H. Yamanaka, O. Sakata, H. Kitagawa, *Nat. Mater.* **2010**, *9*, 565 – 571; f) M. Kondo, S. Furukawa, K. Hirai, S. Kitagawa, *Angew. Chem. Int. Ed.* **2010**, *49*, 5327 – 5330; *Angew. Chem.* **2010**, *122*, 5455 – 5458; g) N. Yanai, S. Granick, *Angew. Chem. Int. Ed.* **2012**, *51*, 5638 – 5641; *Angew. Chem.* **2012**, *124*, 5736 – 5739; h) P. Deria, W. Bury, I. Hod, C. W. Kung, O. Karagiaridi, J. T. Hupp, O. K. Farha, *Inorg. Chem.* **2015**, *54*, 2185 – 2192; i) C. V. McGuire, R. S. Forgan, *Chem. Commun.* **2015**, *51*, 5199 – 5217.

[11] M. C. Daniel, D. Astruc, *Chem. Rev.* **2004**, *104*, 293 – 346.

[12] a) C. Wang, Z. Xie, K. E. deKrafft, W. Lin, *J. Am. Chem. Soc.* **2011**, *133*, 13445 – 13454; b) L. Valenzano, B. Civalleri, S. Chavan, S. Bordiga, M. H. Nilsen, S. Jakobsen, K. P. Lillerud, C. Lamberti, *Chem. Mater.* **2011**, *23*, 1700 – 1718; c) see Ref. [8b]; d) C. Wang, J.-L. Wang, W. Lin, *J. Am. Chem. Soc.* **2012**, *134*, 19895 – 19908; e) H.-L. Jiang, D. Feng, T.-F. Liu, J.-R. Li, H.-C. Zhou, *J. Am. Chem. Soc.* **2012**, *134*, 14690 – 14693; f) D. Feng, Z.-Y. Gu, J.-R. Li, H.-L. Jiang, Z. Wei, H.-C. Zhou, *Angew. Chem. Int. Ed.* **2012**, *51*, 10307 – 10310; *Angew. Chem.* **2012**, *124*, 10453 – 10456; g) W. Morris, B. Volosskiy, S. Demir, F. Gándara, P. L. McGrier, H. Furukawa, D. Cascio, J. F. Stoddart, O. M. Yaghi, *Inorg. Chem.* **2012**, *51*, 6443 – 6445; h) see Ref. [8c]; i) M. Kim, S. M. Cohen, *CrystEngComm* **2012**, *14*, 4096 – 4104; j) D. Feng, W.-C. Chung, Z. Wei, Z.-Y. Gu, H.-L. Jiang, Y.-P. Chen, D. J. Darensbourg, H.-C. Zhou, *J. Am. Chem. Soc.* **2013**, *135*, 17105 – 17110; k) J. E. Mondloch, W. Bury, D. Fairen-Jimenez, S. Kwon, E. J. DeMarco, M. H. Weston, A. A. Sarjeant, S. T. Nguyen, P. C. Stair, R. Q. Snurr, O. K. Farha, J. T. Hupp, *J. Am. Chem. Soc.* **2013**, *135*, 10294 – 10297; l) S. Pullen, H. Fei, A. Orthaber, S. M. Cohen, S. Ott, *J. Am. Chem. Soc.* **2013**, *135*, 16997 – 17003; m) H. Furukawa, F. Gándara, Y.-B. Zhang, J. Jiang, W. L. Queen, M. R. Hudson, O. M. Yaghi, *J. Am. Chem. Soc.* **2014**, *136*, 4369 – 4381; n) H. Fei, S. M. Cohen, *Chem. Commun.* **2014**, *50*, 4810 – 4812.

[13] J. H. Cavka, S. Jakobsen, U. Olsbye, N. Guillou, C. Lamberti, S. Bordiga, K. P. Lillerud, *J. Am. Chem. Soc.* **2008**, *130*, 13850 – 13851.

[14] X. L. Lv, M. M. Tong, H. L. Huang, B. Wang, L. Gan, Q. Y. Yang, C. L. Zhong, J. R. Li, *J. Solid State Chem.* **2015**, *223*, 104 – 108.

[15] a) C. Queffélec, M. Petit, P. Janvier, D. A. Knight, B. Bujoli, *Chem. Rev.* **2012**, *112*, 3777 – 3807; b) G. Guerrero, J. G. Alauzun, M. Granier, D. Laurencin, P. H. Mutin, *Dalton Trans.* **2013**, *42*, 12569 – 12585; c) see Ref. [10h].

[16] a) D. J. Maclachlan, K. R. Morgan, *J. Phys. Chem. Us.* **1992**, *96*, 3458 – 3464; b) K. Segawa, Y. Nakajima, S. Nakata, S. Asaoka, H. Takahashi, *J. Catal.* **1986**, *101*, 81 – 89.

[17] P. Ghosh, Y. J. Colon, R. Q. Snurr, *Chem. Commun.* **2014**, *50*, 11329 – 11331.

[18] a) W. Morris, C. J. Doonan, H. Furukawa, H. Banerjee, O. M. Yaghi, *J. Am. Chem. Soc.* **2008**, *130*, 12626 – 12627; b) M. J. Ingleson, J. P. Barrio, J. B. Guilbaud, Y. Z. Khimyak, M. J. Rosseinsky, *Chem. Commun.* **2008**, 2680 – 2682.

[19] a) C. A. Mirkin, R. L. Letsinger, R. C. Mucic, J. J. Storhoff, *Nature* **1996**, *382*, 607 – 609; b) R. Shenhar, T. B. Norsten, V. M. Rotello, *Adv. Mater.* **2005**, *17*, 657 – 669; c) M. Niederberger, H. Colfen, *Phys. Chem. Chem. Phys.* **2006**, *8*, 3271 – 3287; d) Y. J. Min, M. Akbulut, K. Kristiansen, Y. Golan, J. Israelachvili, *Nat. Mater.* **2008**, *7*, 527 – 538.

[20] S. Horike, S. Shimomura, S. Kitagawa, *Nat. Chem.* **2009**, *1*, 695 – 704.

[21] S. Linic, P. Christopher, D. B. Ingram, *Nat. Mater.* **2011**, *10*, 911 – 921.

Received: July 24, 2015
Revised: September 23, 2015
Published online: October 23, 2015

